Article

Neuron

Touch Receptor-Derived Sensory Information Alleviates Acute Pain Signaling and Fine-Tunes Nociceptive Reflex Coordination

Highlights

- Identification of an A-fiber nociceptor subpopulation that mediates pinprick pain
- Tactile sensory input alleviates A-fiber nociceptor-evoked pain
- Tactile sensory input is required for nociceptive reflex coordination
- Pinprick-evoked paw withdrawal reflex is triggered independently of firing frequency

Authors

Alice Arcourt, Louise Gorham, Rahul Dhandapani, ..., Carmen Birchmeier, Paul A. Heppenstall, Stefan G. Lechner

Correspondence

stefan.lechner@pharma.uni-heidelberg.de

In Brief

Arcourt et al. utilize optogenetics to decipher the role of touch receptors and nociceptors in pain signaling. This approach reveals that tactile sensory input has an analgesic effect on acute pain and is required for normal coordination of nocifensive behavior.

Arcourt et al., 2017, Neuron *93*, 1–15
January 4, 2017
http://dx.doi.org/10.1016/j.neuron.2016.11.027

CellPress

Please cite this article in press as: Arcourt et al., Touch Receptor-Derived Sensory Information Alleviates Acute Pain Signaling and Fine-Tunes Nociceptive Reflex Coordination, Neuron (2016), http://dx.doi.org/10.1016/j.neuron.2016.11.027

Neuron
Article

Touch Receptor-Derived Sensory Information Alleviates Acute Pain Signaling and Fine-Tunes Nociceptive Reflex Coordination

Alice Arcourt,[1] Louise Gorham,[1] Rahul Dhandapani,[2] Vincenzo Prato,[1] Francisco J. Taberner,[1] Hagen Wende,[1,3] Vijayan Gangadharan,[1] Carmen Birchmeier,[3] Paul A. Heppenstall,[2] and Stefan G. Lechner[1,4,*]
[1]Institute of Pharmacology, Heidelberg University, Im Neuenheimer Feld 366, 69120 Heidelberg, Germany
[2]EMBL Monterotondo, Via Ramarini 32, 00016 Monterotondo, Italy
[3]Max-Delbrueck-Center (MDC) for Molecular Medicine, Robert-Roessle-Strasse 10, 13125 Berlin, Germany
[4]Lead Contact
*Correspondence: stefan.lechner@pharma.uni-heidelberg.de
http://dx.doi.org/10.1016/j.neuron.2016.11.027

SUMMARY

Painful mechanical stimuli activate multiple peripheral sensory afferent subtypes simultaneously, including nociceptors and low-threshold mechanoreceptors (LTMRs). Using an optogenetic approach, we demonstrate that LTMRs do not solely serve as touch receptors but also play an important role in acute pain signaling. We show that selective activation of neuropeptide Y receptor-2-expressing (*Npy2r*) myelinated A-fiber nociceptors evokes abnormally exacerbated pain, which is alleviated by concurrent activation of LTMRs in a frequency-dependent manner. We further show that spatial summation of single action potentials from multiple NPY2R-positive afferents is sufficient to trigger nocifensive paw withdrawal, but additional simultaneous sensory input from LTMRs is required for normal well-coordinated execution of this reflex. Thus, our results show that combinatorial coding of noxious and tactile sensory input is required for normal acute mechanical pain signaling. Additionally, we established a causal link between precisely defined neural activity in functionally identified sensory neuron subpopulations and nocifensive behavior and pain.

INTRODUCTION

Sensory stimuli impinging on our skin are detected and encoded by peripheral sensory neurons that can be broadly classified into low-threshold mechanoreceptors (LTMRs), which detect innocuous tactile stimuli, and nociceptors, which exclusively respond to noxious or potentially harmful stimuli. Both populations comprise several subpopulations that respond to mechanical stimuli (>90%), but exhibit different response properties, axonal conduction velocities (CVs), and activation thresholds (Abraira and Ginty, 2013; Dubin and Patapoutian, 2010; Lechner and Lewin, 2013; Lewin and Moshourab, 2004). Accordingly, noxious mechanical stimuli inevitably activate multiple sensory afferent subtypes, including nociceptors and LTMRs, thereby generating a plethora of sensory information that is simultaneously transmitted to the spinal cord. This has raised the question as to whether pain signaling involves the processing and integration of sensory input from multiple afferent subtypes or whether different sensations of pain are generated by activity in so-called labeled lines, i.e., single sensory neuron subpopulations that are particularly sensitive to certain types of sensory stimuli (Ma, 2010; Prescott et al., 2014). Several studies have shown that under certain pathological pain conditions, touch receptor-derived sensory information indeed contributes to the generation of pain. After nerve injury, LTMRs activate nociceptive projection neurons in the dorsal horn of the spinal cord (Sandkühler, 2009), which results in touch-evoked pain (i.e., mechanical allodynia). The spinal interneurons that normally inhibit this sensory modality crosstalk have recently been identified (Duan et al., 2014). However, whether LTMR-derived sensory input is also involved in acute pain signaling in healthy individuals, as originally proposed by the gate control theory of pain (Braz et al., 2014; Melzack and Wall, 1965), is still unclear. Here we utilized optogenetics to enable selective activation of nociceptors and LTMRs in order to decipher their contribution to acute mechanically evoked pain.

RESULTS

To enable selective activation of different primary afferent subtypes, we targeted the expression of the light-activated ion channel Channelrhodopsin-2 (ChR2) to genetically defined sensory neuron subpopulations. To this end, we crossed ChR2-EYFP$^{loxP/+}$ mice (Madisen et al., 2012) with various different Cre-driver lines, including *SNS*^{Cre}, *Trpv1*^{Cre}, *c-Maf*^{Cre}, *MafA*^{Cre}, and *Npy2r*^{Cre}, and examined ChR2 expression patterns by probing light sensitivity of functionally identified cutaneous afferents using single-unit teased fiber recordings in an in vitro skin-nerve preparation. Two mouse lines, the *Npy2r*$^{Cre/+}$*;ChR2-EYFP*$^{loxP/+}$ and *MafA*$^{Cre/+}$*; ChR2-EYFP*$^{loxP/+}$ lines, hereafter termed *Npy2r*^{ChR2} and *MafA*^{ChR2}, respectively, proved particularly useful for studying crosstalk of nociceptors and LTMRs in acute pain signaling. In *SNS*^{ChR2}, *Trpv1*^{ChR2}, and *c-Maf*^{ChR2} mice, ChR2

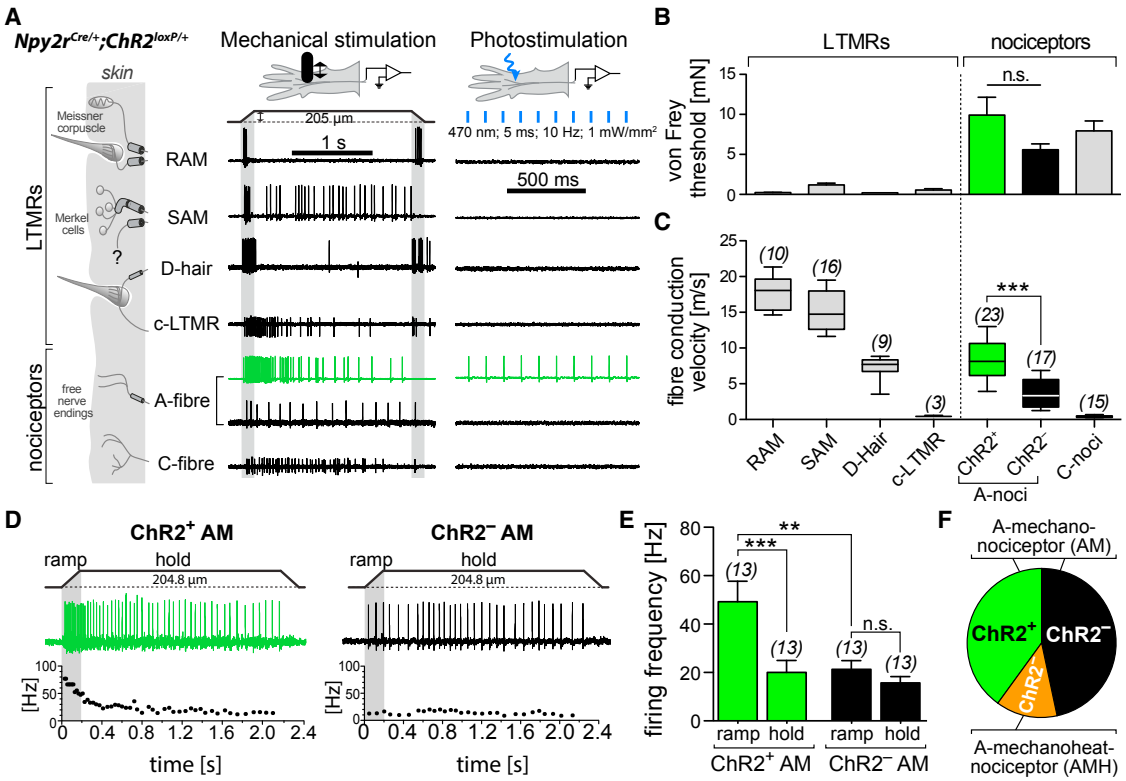

Figure 1. In *Npy2r*^{ChR2} Mice, Photostimulation Selectively Activates a Subset of A-Fiber Mechanonociceptors

(A) Typical AP responses of the depicted afferent subtypes (left) evoked by mechanical ramp-and-hold stimuli (middle) and by 10 Hz photostimulation (right).

(B) Minimal force required to activate the indicated afferent subtypes (bars represent means ± SEM).

(C) CVs of the indicated afferent subtypes (solid line in box represents means; whiskers show 10–90 percentile; numbers in brackets indicate the number of examined afferents; $p < 0.001$, Student's t test).

(D) Typical responses (middle) of ChR2$^+$ (left panel) and ChR2$^-$ A-fiber mechanonociceptors (right panel) evoked by mechanical stimulation (top). Instantaneous firing frequency of each AP is plotted at the bottom. Additional examples are shown in Figures S1A and S1B.

(E) Comparison of the mean instantaneous firing frequency ± SEM during the ramp phase and the hold phase of ChR2$^+$ A-fiber mechanonociceptors (green) and ChR2$^-$ A-fiber mechanonociceptors (black). Numbers in brackets indicate N numbers. Ramp versus hold frequencies from the same population were compared using a paired t test. Ramp frequencies of ChR2$^+$ and ChR2$^-$ A-fiber mechanonociceptors were compared using Student's t test (***$p < 0.001$; **$p < 0.01$).

(F) Pie chart shows the proportion of ChR2$^+$ A-fiber mechanonociceptors (green), ChR2$^-$ A-fiber mechanonociceptors (black), and heat-sensitive A-fiber nociceptors (AMH, orange).

was expressed in multiple functionally diverse sensory neuron subpopulations, which precluded selective activation of individual afferent subpopulations.

In *Npy2r*^{ChR2} Mice, Photostimulation of the Hindpaw Skin Selectively Activates a Subset of A-Fiber Nociceptors

With the skin-nerve recording technique, functionally distinct primary afferent subtypes can unequivocally be distinguished by means of axonal CV, the minimal mechanical force required to elicit an action potential (AP) (von Frey threshold) and the characteristic firing pattern in response to standardized mechanical ramp-and-hold stimuli (Figures 1A–1C) (Koltzenburg et al., 1997). To examine which type of afferents expresses ChR2 in *Npy2r*^{ChR2} mice, the receptive fields of functionally characterized afferents were exposed to blue light (470 nm). Such photostimuli only evoked APs in a subset of myelinated A-fiber nociceptors—i.e., fibers that are exclusively activated by mechanical stimuli in the noxious range and exhibit fast axonal CVs (Figures 1A–1C). Interestingly, A-fiber nociceptors that were activated by photostimulation (ChR2 positive) significantly differed from light-insensitive A-fiber nociceptors (ChR2 negative) in terms of axonal CVs (Figure 1C) and their firing pattern in response to mechanical stimulation (Figure 1D), suggesting that A-fiber nociceptors comprise two functionally different subpopulations. ChR2-positive afferents exhibited significantly faster CVs than ChR2-negative A-fiber nociceptors (8.47 ± 3.29 m/s versus 3.73 ± 2.15 m/s, $p < 0.001$, Student's t test; Figure 1C). Moreover, ChR2-positive afferents fired APs at significantly higher frequencies during the dynamic phase (ramp) of a mechanical ramp-and-hold stimulus compared to the static phase (hold) (ramp, 49.2 ± 30.6 Hz versus hold, 20.0 ± 17.7 Hz, $p = 0.0003$, paired t test; Figures 1D, 1E, S1A, and S1C, available online), whereas ChR2-negative afferents fired at a constant frequency throughout the entire duration of the mechanical stimulus (ramp, 21.3 ± 12.8 Hz versus hold,

15.7 ± 9.2 Hz, p = 0.084; Figures 1D, 1E, S1B, and S1C). The difference between firing frequencies during the dynamic and static phase of the mechanical stimulus was not only statistically significant when comparing the means of the entire population (Figure 1E), but was also highly significant when comparing the mean instantaneous firing frequency during the ramp and the hold phase of individual ChR2-expressing fibers (Figure S1D).

A more detailed functional characterization revealed that NPY2R-ChR2-positive afferents constitute a subset of so-called A-fiber mechanonociceptors—i.e., myelinated A-fiber nociceptors that exclusively responded to noxious mechanical stimuli, but not to heat or capsaicin (Figure S1E), and accordingly did not express the heat- and capsaicin-sensitive ion channel TRPV1 (Figure S1F) (Caterina et al., 1997). In agreement with previous studies, only a small proportion of A-fiber nociceptors responded to noxious heat (Figures 1F and S1E) (Cain et al., 2001; Koltzenburg et al., 1997; Lawson et al., 2008), but none of these afferents were activated by photostimulation.

Lumbar NPY2R-ChR2-Positive Sensory Neurons Express Neurochemical Markers of Peptidergic A-Fiber Nociceptors

The results from the electrophysiological characterization were quite unexpected; they contradict the data reported by Li and colleagues (2011), who showed that GFP-positive sensory afferents in an *Npy2r*^{GFP} BAC-transgenic reporter mouse line form lanceolate endings around hair follicles, which is characteristic of Aβ-fiber RA-LTMRs. Hence, to corroborate our findings, we next examined co-expression of well-described neurochemical subpopulation markers with ChR2 in sections of L3-L5 lumbar dorsal root ganglia (DRG). Consistent with our functional analysis, we observed ChR2 expression in 32% of all putative A-fiber nociceptors—i.e., neurons that co-express the neurofilament-heavy polypeptide (*Nefh*), a marker of myelinated neurons, and the nerve growth factor receptor TRKA, a peptidergic nociceptor marker (Figures 2A–2C and 2G). The vast majority of ChR2-positive neurons (75%; 620/824) belonged to this subpopulation of sensory neurons and accordingly also expressed the neuropeptide calcitonin gene-related peptide (CGRP) (Figure S2A), which is known to be expressed in almost all TRKA-expressing sensory neurons (Averill et al., 1995). Peptidergic C-fiber nociceptors (NEFH$^-$/TRKA$^+$ neurons; Figures 2A and 2G) and non-peptidergic C-fiber nociceptors (IB4$^+$ neurons; Figures 2D and 2G) did not express ChR2. Furthermore, we observed ChR2 expression in a small number of putative LTMRs, which mediate the sense of touch. Hence, 5.6% of the neurons that express the Aβ-fiber RA-LTMR marker calbindin (Wende et al., 2012) and 4.3% of the cells expressing the neurotrophin receptor TRKB, which is expressed in D-hair mechanoreceptors and at low levels in RA-LTMRs (Rutlin et al., 2014; Wende et al., 2012), were ChR2 positive (Figures 2B, 2E, and 2G). The GDNF receptor RET, which is expressed in non-peptidergic nociceptors (Molliver et al., 1997) but also in some LTMRs, including RA-LTMRs and Aβ-field receptors (Bai et al., 2015; Luo et al., 2009), was only present in a small subset of ChR2-positive neurons (Figure S2B). Parvalbumin (PV), a proprioceptor marker, and TRKC, which is expressed in some LTMRs and proprioceptors (Bai et al., 2015; Ernfors et al., 1994), were not detected in ChR2-positive neurons (Figures 2C and 2F). Importantly, ChR2-positive neurons exhibited high levels of Npy2r mRNA, indicating the expression of *Npy2r* in these cells (Figure S2C). Additionally, patch-clamp recordings revealed that ChR2-positive neurons express the tetrodotoxin (TTX)-resistant voltage-gated sodium channel Nav1.8 (Figures S2D–S2F), which is expressed in most nociceptors (Akopian et al., 1999).

NPY2R-ChR2-Positive Afferents Terminate as Free Nerve Endings in the Hairy and Glabrous Hindpaw Skin

We next examined the peripheral and central projection patterns of ChR2-expressing neurons in *Npy2r*^{ChR2} mice. In the hindpaw skin, ChR2-positive afferents terminated as myelinated (NEFH$^+$) free nerve endings (Figure 3A), which are characteristic of nociceptive sensory afferents (Basbaum et al., 2009; Dubin and Patapoutian, 2010). By contrast, sensory end organs of LTMRs were not innervated by ChR2-expressing fibers. Thus, lanceolate endings and circumferential endings around hair follicles (Figures 3B and 3C), which represent Aβ RA-LTMRs (Li et al., 2011) and Aβ field-LTMRs (Bai et al., 2015), respectively, did not show ChR2-EYFP immunoreactivity. Furthermore, afferents that innervate Meissner corpuscles, which are the sensory end organs of Aβ RA-LTMRs in the glabrous skin, and fibers that innervate Merkel cells (Aβ SA1-LTMRs) (Maricich et al., 2009), also did not express ChR2 (Figures 3D and S3B). Consistent with the morphology of their cutaneous terminals, the central projections of ChR2-positive sensory neurons predominantly terminated in lamina II of the lumbar spinal cord (Figure 3E), which is known to be involved in processing pain-related information and receives input from A-fiber nociceptors (Braz et al., 2014; Todd, 2010). These peripheral and central projection patterns are consistent with the functional properties (Figure 1) and the neurochemical marker profile (Figure 2), which also indicate that NPY2R-ChR2-positive sensory neurons constitute a subset of peptidergic A-fiber nociceptors. This is further supported by a recent large-scale single-cell RNA sequencing study that also describes *Npy2r* expression in A-fiber nociceptors (Usoskin et al., 2015) and a previous report showing that *Npy2r* is expressed in medium to large CGRP-positive nociceptors in lumbar rat DRGs (Zhang et al., 1997). However, as indicated above, our observations differ from the results reported by Li and colleagues (2011), who showed that GFP-positive sensory afferents in an *Npy2r*^{GFP} BAC-transgenic reporter mouse line form lanceolate endings around hair follicles, which is characteristic of Aβ-fiber RA-LTMRs. It should be noted, however, that Li and colleagues examined innervation of the hairy back skin of the trunk, whereas we investigated hairy and glabrous hindpaw skin. To address this issue, we examined innervation of hairy back skin by NPY2R-ChR2-positive fibers. Indeed, in the back skin we encountered ChR2-positive lanceolate endings around guard hairs, but the vast majority of ChR2-positive fibers also terminated as free nerve endings in the epidermis (Figures S3A and S3B). To test whether the Npy2r-ChR2-positive free nerve endings indeed originate from sensory neurons and not from sympathetic neurons or local cells in the skin, we next injected the lumbar L3 and L4 DRGs of *Npy2r*^{Cre} mice with an AAV virus encoding the fluorescent reporter EYFP flanked by loxP sites (Figure S3C). Three weeks after virus injection,

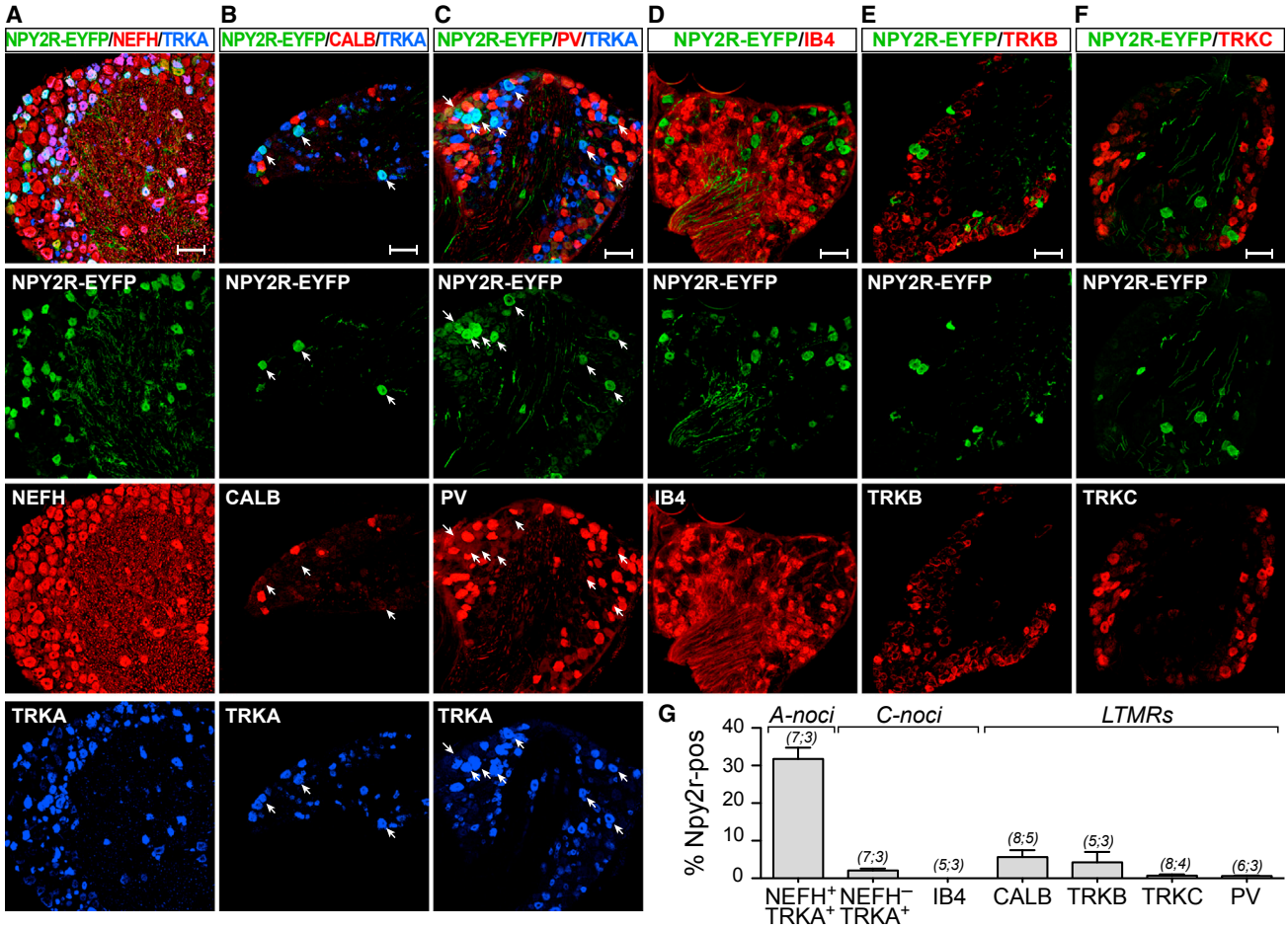

Figure 2. In *Npy2r*^{ChR2} Mice, ChR2-EYFP Expression Is Confined to a Subset of Myelinated TRKA-Expressing Neurons

(A–F) Immunostaining of L3-L5 DRGs from *Npy2r*^{ChR2} mice to examine expression of ChR2-EYFP (NPY2R-EYFP) in TRKA-positive peptidergic nociceptors (A), CALB-positive RA-LTMRs (B), PV-positive proprioceptors (C), IB4-binding non-peptidergic nociceptors (D), TRKB-positive D-hair mechanoreceptors and RA-LTMRs (E), and TRKC-positive LTMRs (F). Scale bar, 100 μm in all images.

(G) Percentage of neurons from the neurochemically defined subpopulation indicated at the bottom that co-express ChR2-EYFP. Bars represent means ± SD of five to eight DRGs from at least three different mice.

we observed dense arrays of EYFP-positive free nerve endings in hairy and glabrous hindpaw skin (Figures 3F and 3G), demonstrating that NPY2R-Cre-positive neurons indeed terminate as free nerve endings in the skin. Co-staining with DAPI suggested that these EYFP-positive free nerve endings terminate in and beyond the stratum spinosum of the epidermis (i.e., layer with particularly high density of keratinocyte nuclei) (Figures 3F and 3G). This observation is consistent with a previous report showing that free nerve endings of sensory neurons with large axons terminate between ~10 μm and 70 μm below the skin surface (Wu et al., 2012). To further confirm this observation, we also counterstained skin sections for integrin α6, which is predominantly expressed in the stratum basale of the epidermis and thus allows unequivocal visualization of the dermal-epidermal junction (Georges-Labouesse et al., 1996; Sonnenberg et al., 1991). Indeed, NPY2R-ChR2-positive free nerve endings cross the dermal-epidermal junction and terminate in the epidermis (Figure S3D).

Taken together, our immunohistochemical characterization demonstrates that NPY2R-ChR2-positive fibers terminate as free nerve endings in the epidermis of the hairy and glabrous skin of the hindpaw, which is characteristic of nociceptive afferents, whereas they form both free nerve endings and lanceolate endings around guard hairs in the hairy back skin. This peripheral nerve terminal morphology of hindpaw afferents is consistent with the neurochemical marker profile found in lumbar DRGs and, together with the functional data from the skin-nerve recordings, strongly suggests that NPY2R-ChR2-positive afferents innervating the paw skin constitute a subset of peptidergic myelinated A-fiber nociceptors.

Npy2r^{Cre}-Positive Afferents Are Required for Pinprick-Evoked Withdrawal Reflexes

Given the fast axonal CVs, the high mechanical thresholds, and the vigorous AP firing during the initial phase of noxious skin indentation, we speculated that NPY2R-Cre-positive A-fiber

mechanonociceptors may be involved in acute pain signaling and could play an important role in the rapid and efficient execution of protective nociceptive paw withdrawal reflexes. To directly test this hypothesis, we assessed nociceptive reflexes in mice lacking NPY2R-Cre-positive sensory neurons. DRG-specific ablation of NPY2R-Cre-positive neurons was achieved by crossing *Npy2r*$^{Cre/+}$ mice with *Avil*$^{iDTR/+}$ mice, which express the diphtheria toxin receptor (DTR) with an upstream loxP-STOP-loxP cassette under control of the DRG-specific Advillin promoter (Stantcheva et al., 2016). Following diphtheria toxin (DTX) injections, the number of NPY2R-Cre-positive neurons was reduced by ~75%, as confirmed by anti-iDTR immunolabeling, and the remaining cells only showed very weak DTR immunoreactivity (Figure 4A). Strikingly, after ablation of NPY2R-Cre-positive DRG neurons, paw withdrawals in response to pinprick stimuli were significantly delayed (Figure 4B; Movie S1). Withdrawal reflexes in response to von Frey stimuli and to noxious heat were not altered (Figure 4B), indicating that motor neurons and spinal interneurons, such as somatostatin-expressing interneurons that are required for both pinprick- and von Frey-evoked withdrawal reflexes (Duan et al., 2014), were not ablated. Moreover, DTX-treated littermate controls that did not express DTR showed normal pinprick-evoked paw withdrawals (Figure 4B), demonstrating that DTX treatment per se does not affect nociceptor sensitivity or other physiological processes that might alter reaction time. Thus, our data show that NPY2R-Cre-positive neurons are required for the rapid and efficient execution of pinprick-evoked paw withdrawal reflexes.

In Vivo Photostimulation of *Npy2r*^{ChR2} Mice Evokes Pain Behavior in a Frequency-Dependent Manner

We next asked whether selective activation of NPY2R-ChR2-positive afferents is also sufficient to trigger nociceptive withdrawal reflexes and pain. In vitro skin-nerve recordings had shown that light pulses with durations of 5 ms are most suitable to precisely control spike timing because they consistently evoked only a single AP, whereas longer light pulses triggered brief bursts with unpredictable numbers of APs. This was the case when photostimuli were applied to the corium side of the skin as well as when stimuli were applied to the epidermis (Figure S4). Thus, using repeated stimulation with 5 ms light pulses, we were able to reliably generate trains of APs with frequencies of up to 20 Hz in ChR2-expressing A-fiber mechanonociceptors (Figure S4). In vivo photostimulation of the plantar surface of the hindpaw evoked a wide range of robust pain behaviors in *Npy2r*$^{Cre/+}$;*ChR2*$^{loxP/+}$ mice (Movies S2 and S3), but not in *Npy2r*$^{+/+}$;*ChR2*$^{loxP/+}$ littermate controls (Movie S3). The incidence of guarding (persistently keeping the paw lifted after stimulation), jumping, and audible vocalization, which indicate a conscious awareness of pain (Mogil, 2009), increased with stimulation frequency, whereas paw withdrawal occurred at all tested frequencies (Figure 4C). Interestingly, even a single 5 ms light pulse consistently evoked robust paw withdrawal and, in some cases, guarding and jumping (Figure 4C; Movie S4).

The fact that a single 5 ms light pulse was sufficient to trigger paw withdrawal, plus the remarkable intensity of the observed behavioral responses, raised the questions of whether selective activation of nociceptors results in abnormally exacerbated pain and whether additional sensory input is required to produce pain behavior comparable to that evoked by noxious mechanical stimuli. Indeed, the gate control theory of pain (Melzack and Wall, 1965) proposes that nociceptor input to nociceptive transmission neurons in the spinal cord is inhibited by concurrent input from LTMRs, which are inevitably activated by naturally occurring noxious mechanical stimuli.

MafA^{ChR2} Mice Enable Selective Activation of LTMRs

To directly test this hypothesis, we generated a *MafA*^{Cre} mouse line to enable selective optogenetic control of LTMRs (Figure S5A). *MafA* is a transcription factor that is specifically expressed in LTMRs (Bourane et al., 2009; Wende et al., 2012). Accordingly, in *MafA*^{ChR2} mice, ChR2-positive lumbar DRG neurons co-expressed neurochemical markers of LTMRs, but not nociceptor markers. More precisely, 74% (246/334) of the neurons that express calbindin, a marker for Aβ RA-LTMRs (Wende et al., 2012), co-expressed ChR2 (Figures 5A and 5F), and 38% (208/547) of the TRKB-positive neurons, which represent Aδ-fiber D-hair mechanoreceptors and Aβ RA-LTMRs (Rutlin et al., 2014; Wende et al., 2012), were also ChR2 positive (Figures 5B and 5F). Furthermore, a small proportion of TRKC-positive neurons (26%; 100/383) also exhibited ChR2-EYFP immunoreactivity (Figures 5C and 5F). By contrast, neither NEFH$^+$/TRKA$^+$ double-positive neurons (Figure 5E), which represent A-fiber nociceptors, nor peptidergic C-fiber nociceptors (NEFH$^-$/TRKA$^+$; Figure 5E) or non-peptidergic C-fiber nociceptors (IB4$^+$; Figure 5D) expressed ChR2. Consistent with the neurochemical marker profile of MAFA-ChR2-positive neurons, photostimulation of the skin only evoked APs in Aβ-fiber RA-LTMRs (7/7), in some Aδ-fiber D-hair mechanoreceptors (4/11), and in a subset of Aβ-fiber SA-LTMRs (10/25) (Figures 5G–5I). Neither A-fiber nor C-fiber nociceptors were activated by photostimulation (Figures 5G–5I).

We next examined the peripheral and central projection patterns of MAFA-ChR2-expressing neurons. MAFA-ChR2-positive fibers formed lanceolate endings around hair follicles (Figures 6A and 6D) and innervated S100-positive Meissner corpuscles in the dermal papillae of the hindpaw footpads (Figure 6B), which are the typical end organs of Aβ RA-LTMRs in the hairy and glabrous skin, respectively (Abraira and Ginty, 2013). Identical peripheral projections were observed in whole mount skin stainings using Z/AP reporter mice (Figures S5B and S5C). NEFH-positive fibers that innervate TROMA1-positive Merkel cells—i.e., Aβ SA1-LTMRs—did not express ChR2 (Figure 6C). Importantly, NEFH-positive free nerve endings (A-fiber nociceptors; Figure 6D) and PGP9.5-positive free nerve endings (Figure 6E), which include A-fiber and C-fiber nociceptors, also did not express ChR2. Hence, our data demonstrate that in *MafA*^{ChR2} mice, ChR2 expression is confined to LTMRs. Consistent with this, ChR2-EYFP immunoreactivity was predominantly observed in laminae III-IV (Figure 6F), which are known to receive input from Aβ-LTMRs (Li et al., 2011). It should, however, be noted that *MafA* is also expressed in some local interneurons in lamina III-IV (Del Barrio et al., 2013) and thus we cannot rule out that some of the ChR2-EYFP immunofluorescence in these laminae is generated by these cells. However, most importantly, ChR2-EYFP immunoreactivity is largely absent from the superficial dorsal horn, which receives input from nociceptors. The few

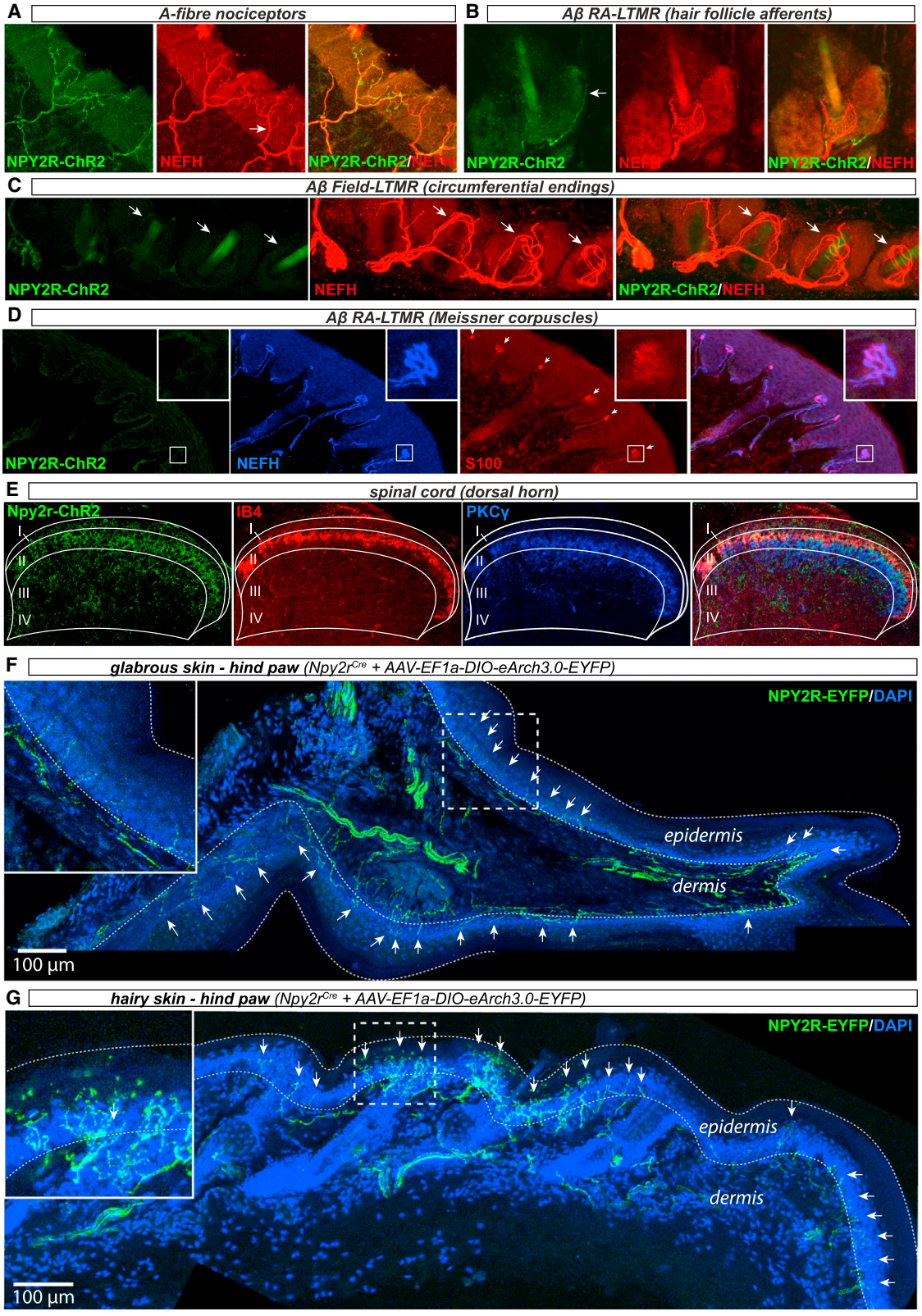

(legend on next page)

projections observed in inner lamina II most likely originate from TRKB-positive D-hair mechanoreceptors, which are known to project to lamina IIi (Li et al., 2011), and some of which also express ChR2 (Figure 5F).

LTMR Input Alleviates Acute A-Fiber Nociceptor-Evoked Pain

We next tested whether concurrent activation of LTMRs and A-fiber nociceptors evokes different pain behaviors compared to selective activation of A-fiber nociceptors. To this end, we crossed *Npy2r*^{ChR2} mice with *MafA*^{ChR2} mice. Strikingly, only one from seven *Npy2r*^{ChR2};*MafA*^{ChR2} double transgenic mice briefly squeaked, whereas all *Npy2r*^{ChR2} mice vocalized for several seconds in response to photostimulation at frequencies above 5 Hz (Figure 7A; Movies S2 and S3). Furthermore, the stimulation frequencies required to evoke jumping and guarding were much higher in *Npy2r*^{ChR2};*MafA*^{ChR2} mice as compared to *Npy2r*^{ChR2} mice (Figure 7A). *MafA*^{ChR2} mice never jumped or vocalized in response to photostimulation (data not shown), though they did occasionally withdraw the paw (see next section). In general, the analgesic effect of LTMR activation was stronger at low stimulation frequencies (compare pain scores in Figure S6A), which is consistent with the gate control theory, which proposed that the inhibitory effect of LTMR input on pain transmission is blocked as nociceptor activity increases. To obtain additional evidence for the analgesic effect of concurrent LTMR input, we next examined induction of the immediate early gene *c-Fos*—an indicator of neuronal activity—in neurons in lamina I of the spinal dorsal horn. Lamina I contains the majority of projection neurons that relay noxious information to higher brain regions and are thus important for the conscious perception of pain (Todd, 2010). Consistent with the behavioral tests, 5 Hz photostimulation induced *c-Fos* expression in significantly more cells in lamina I of the ipsilateral dorsal horn of *Npy2r*^{ChR2} mice than of *Npy2r*^{ChR2};*MafA*^{ChR2} double transgenic mice (7.3 ± 1.0 cells/section versus 3.6 ± 0.5 cells/section, $p < 0.05$; one-way ANOVA, Dunn's multiple comparison test; Figures 7B and 7C). Selective activation of LTMRs (*MafA*^{ChR2}) did not induce significant *c-Fos* activation as compared to controls (*ChR2*$^{loxP/+}$ mice) (Figures 7C and S6C). In the contralateral dorsal horn, significant *c-Fos* activation was not observed in any of the tested mouse lines (Figures S6B and S6C).

LTMR Input Is Required for Well-Coordinated Reflex Execution

Interestingly, simultaneous activation of LTMRs and A-fiber nociceptors changed neither the incidence (Figure 7A) nor the latency (Figures 8A, 8B, and 8D) of single light pulse-evoked paw withdrawals, suggesting that LTMR input only gates pain signaling, not nociceptive reflex encoding. In *Npy2r*^{ChR2} and *Npy2r*^{ChR2};*MafA*^{ChR2} mice, a single 5 ms light pulse consistently (100% of the trials) evoked instantaneous ipsilateral paw withdrawal with almost identical and remarkably short latencies (26.5 ± 3.5 ms in *Npy2r*^{ChR2} and 24.3 ± 1.5 ms in *Npy2r*^{ChR2};*MafA*^{ChR2}; Figure 8D; Movies S4 and S5), indicating that photostimulation-evoked paw withdrawal was mediated by a spinal reflex arc in both mouse lines. In *MafA*^{ChR2} mice, photostimulation also occasionally evoked paw withdrawal (61% of the trials; Movie S6); however, these withdrawals occurred with about ten times longer latencies (208 ± 47 ms; Figure 8D), which, considering the fast axonal CVs of Aβ-LTMRs, suggests that these withdrawals were not triggered by a spinal reflex arc but were instead initiated by higher brain regions in response to an unexpected sensory percept. Interestingly, even though concurrent LTMR input did not inhibit single light pulse-evoked paw withdrawals, it appears to be required for fine-tuning reflex coordination. Thus, in *Npy2r*^{ChR2} mice, a single light pulse consistently evoked bilateral paw withdrawal and, in some cases, even jumping with all four paws (Figures 8A and 8D; Movie S4), whereas concurrent activation of nociceptors and LTMRs in *Npy2r*^{ChR2};*MafA*^{ChR2} mice triggered well-coordinated unilateral paw withdrawal (Figures 8B and 8D; Movie S5), which was indistinguishable from withdrawals evoked by noxious mechanical stimuli (e.g., pinprick; Figure 8C; Movie S1).

The observation that a single 5 ms light pulse is sufficient to evoke paw withdrawal was quite unexpected and surprising, as it suggests that paw withdrawal is triggered independently of firing frequency. To further test this hypothesis, we measured the latencies of pinprick-evoked paw withdrawals using a custom-built force measurement system to which a pin was attached (Figures S7A and S7B). With this device, we could precisely determine the point in time at which the pin first contacts the skin as well as the time at which the mouse lifts the paw (Figures 8F and S7B). Moreover, we could accurately measure the stimulation velocity at which the pinprick stimulus was applied. These experiments revealed that pinprick-evoked paw

Figure 3. Peripheral and Central Projections of *Npy2r*^{Cre}-Positive Neurons

(A) NPY2R-ChR2-positive (green) myelinated fibers (NEFH+, red) terminate as free nerve endings in the epidermis. Note that not all NEFH+ free nerve endings express ChR2-EYFP (arrow). These fibers probably represent ChR2^{-} A-fiber nociceptors (see Figure 1).

(B) NPY2R-ChR2-positive fibers do not form NEFH+ lanceolate endings around hair follicles. Note that an NPY2R-ChR2-positive fiber projects up to the epidermis alongside the hair (arrow).

(C) NEFH+ circumferential endings around hair follicles (marked by arrows) do not express Npy2r-ChR2.

(D) Meissner corpuscles (indicated by arrows), visualized by S100 labeling (red), that reside in the dermal papillae of the hindpaw footpad are innervated by NEFH+ (blue) fibers that do not express ChR2 (green). Inset shows magnified view of the typical spiral-shaped innervation of a Meissner corpuscle.

(E) Npy2r-ChR2-positive fibers (green) project to lamina II of the spinal dorsal horn. Lamina IIo was visualized by IB4 staining. PKCγ staining (blue) was used to visualize the border between lamina II and III.

(F and G) L3 and L4 DRGs were injected with AAV-EF1a-DIO-eArch3.0-EYFP. Three weeks after injection, EYFP fluorescence was observed in free nerve endings (marked by arrows) in both glabrous (F) and hairy (G) hindpaw skin. The dashed lines outline the dermal-epidermal junction and the skin surface. The dermal-epidermal junction and the skin surface were identified by packing density of keratinocyte nuclei and the autofluorescence of the stratum corneum, respectively. Note that lanceolate endings around hair follicles were not observed (G). Images shown in (F) and (G) are composite images assembled from multiple high-resolution images.

Scale bars, 50 (A–C) and 100 μm (D–G).

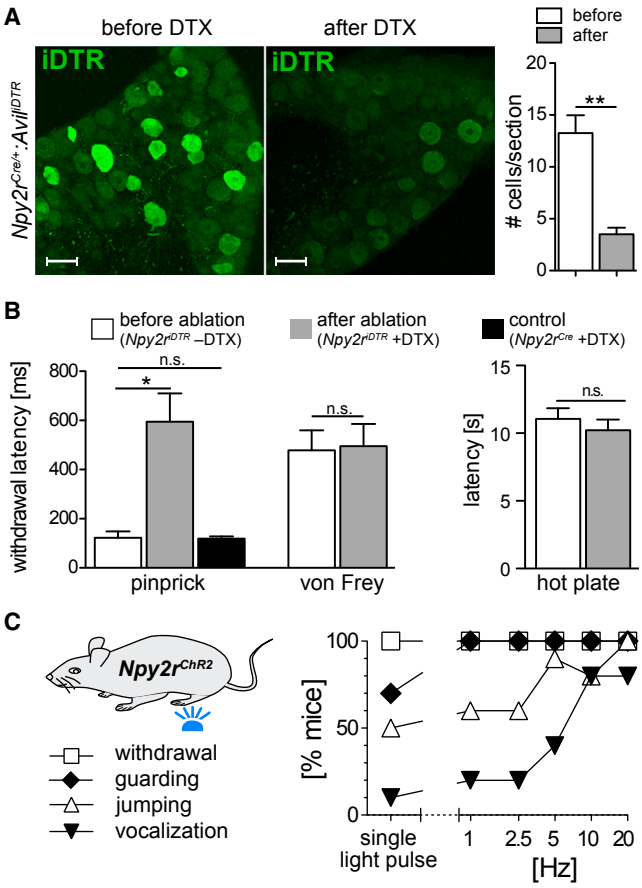

Figure 4. *Npy2r*^{Cre}-Positive Neurons Detect Pinprick Stimuli and Mediate Acute Pain

(A) Diphtheria toxin receptor (DTR) expression in DRGs of *Npy2r*$^{Cre/+}$;*Avil*^{iDTR} mice before (left image) and 7 days after DTX injection (right image). Bar graph shows the number of DTR-positive neurons before and after ablation (mean ± SEM, n = 3 mice, **p < 0.01, Student's t test). Scale bars, 50 μm.

(B) Latencies (mean ± SEM) of withdrawals evoked by the indicated stimuli in the same mice before (white bars) and after (gray bars) ablation (paired t test; N = 5; *p < 0.05). Black bar shows withdrawal delay of DTX-treated littermates that did not express DTR.

(C) Incidence of the indicated behavioral response (percent of mice showing the behavior) as a function of stimulation frequency. Each mouse was stimulated for 10 s.

withdrawals are triggered with a mean latency of 75.3 ± 15.6 ms and an average force of 11.4 ± 2.9 mN (seven mice, three trials per mouse; Figures 8E and S7B). Von Frey filament-evoked paw withdrawal occurred with much longer latencies (328.1 ± 89.7 ms; data not shown). The withdrawal latencies measured with this approach were similar to the latencies measured using slow-motion video imaging (240 fps; Figure 4B). We then examined the latencies of APs evoked by pinprick stimuli applied with the same force and the same velocity in NPY2R-ChR2-positive A-fiber nociceptors. The first AP evoked by such stimuli was fired with a mean latency of 42.2 ± 17.47 ms (Figure 8E), which was comparable to previously described mechanical latencies of A-fiber mechanonociceptors (Milenkovic et al., 2008). More importantly, the latency of the second AP was 94.2 ± 27.9 ms, which is longer than the latency of pinprick-evoked paw withdrawals (~75.3 ms; Figure 8E). Therefore, the second AP is unlikely to contribute to triggering the paw withdrawal reflex, which supports the results from the photostimulation experiments that suggested that paw withdrawal is triggered independently of firing frequency.

DISCUSSION

Taken together, our study reveals a previously unrecognized functional heterogeneity of myelinated nociceptors and identifies a subset of A-fiber mechanonociceptors that is required for pinprick-evoked paw withdrawal reflexes. Furthermore, in demonstrating that concurrent activation of LTMRs alleviates A-fiber mechanonociceptor-evoked pain, we directly confirm one of the central predictions of the gate control theory, which proposed that LTMR input inhibits nociceptive transmission in the spinal dorsal horn (Melzack and Wall, 1965). Finally, we demonstrate that sensory input from LTMRs is required for normal, well-coordinated execution of the nociceptive paw withdrawal reflex.

A-Fiber Mechanonociceptor Heterogeneity

C-fiber nociceptors comprise a variety of subpopulations that are finely tuned to detect different types of noxious physical and chemical stimuli, but little is known about the molecular and functional diversity of A-fiber nociceptors (Basbaum et al., 2009; Dubin and Patapoutian, 2010). In mice, the vast majority of A-fiber nociceptors are exclusively sensitive to mechanical stimuli, termed A-fiber mechanonociceptors, and only a small proportion of A-fiber nociceptors in addition to mechanical stimuli also respond to noxious thermal stimuli (Cain et al., 2001; Koltzenburg et al., 1997; Lawson et al., 2008). The CV distribution of A-fiber mechanonociceptors covers a remarkably wide range (Djouhri and Lawson, 2004)—i.e., 1 m/s to more than 10 m/s in mice—suggesting that fast and more slowly conducting A-fiber mechanonociceptors may serve different physiological roles. However, functional diversity of A-fiber mechanonociceptors has not been described (Koltzenburg et al., 1997; Lawson et al., 2008; Stucky et al., 1999), though a trend toward higher firing frequencies in response to noxious mechanical stimuli has been reported for particularly fast-conducting A-fiber mechanonociceptors (McIlwrath et al., 2007; Woodbury and Koerber, 2003). A possible explanation for the failure to find functional heterogeneity among mouse A-fiber mechanonociceptors is that previous studies have used CV as the primary distinguishing feature to subclassify A-fiber mechanonociceptors into fast-conducting A-fiber mechanonociceptors (sometimes termed Aβ-fiber HTMRs [high-threshold mechanoreceptors]) and more slowly conducting A-fiber mechanonociceptors (usually termed Aδ-fiber mechanonociceptors), which may not be appropriate for the following reasons. First, determining a CV cut-off that allows unequivocal discrimination of Aβ-fiber HTMRs from Aδ-fiber nociceptors is difficult as the CV distribution of A-fiber nociceptors is unimodal and thus has neither a minimum in the range of the commonly used CV cut-off (10 m/s) nor clear peaks in the Aδ- and Aβ-fiber range (Cain et al., 2001; Djouhri and Lawson, 2004; Koltzenburg et al., 1997; Stucky et al., 1999). Second, differences in CVs are not necessarily a prerequisite for functional

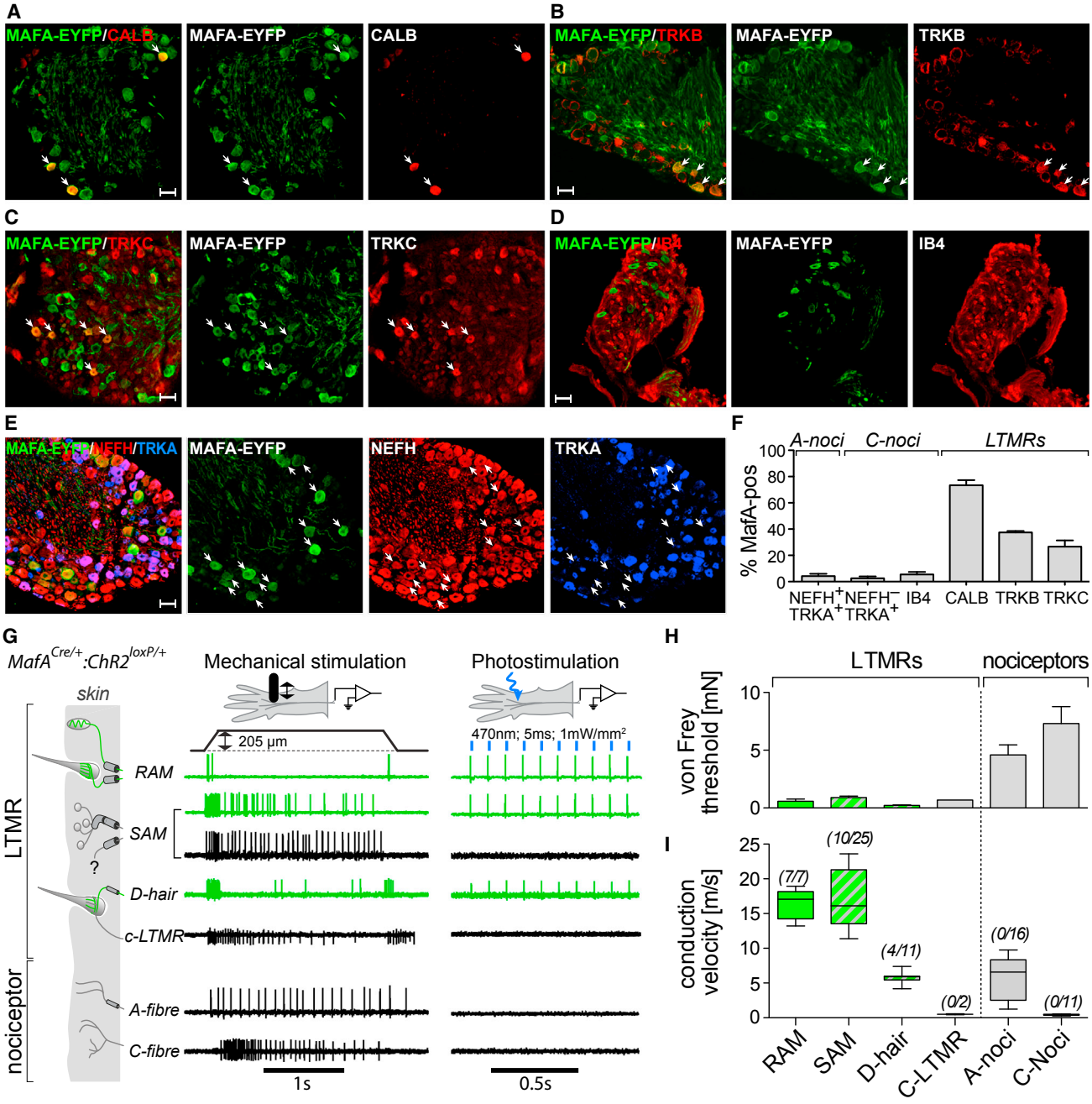

Figure 5. In *MafA*^{ChR2} Mice, ChR2 Expression Is Confined to LTMRs

(A–E) Immunostaining of L3-L5 DRGs from *MafA*^{ChR2} mice to examine expression of ChR2-EYFP (MafA-EYFP) in Calb-positive RA-LTMRs (A), TRKB-positive D-hair mechanoreceptors and RA-LTMRs (B), TRKC-positive LTMRs (C), IB4-binding non-peptidergic nociceptors (D), and TRKA-positive peptidergic nociceptors (E). Scale bars, 50 µm.

(F) Percentage of neurons from the neurochemically defined subpopulation indicated at the bottom that co-express ChR2-EYFP. Bars represent means ± SD of five to eight DRGs from three different mice.

(G) Typical AP responses of the depicted afferent subtypes (left) evoked by mechanical ramp-and-hold stimuli (middle) and by 10 Hz photostimulation (right).

(H) The minimal force required to activate the indicated afferent subtypes (bars represent means ± SEM).

(I) CVs of the indicated afferent subtypes (solid line in box represents means; whiskers show 10–90 percentile; numbers in brackets indicate the number of examined afferents; $p < 0.001$, Student's t test).

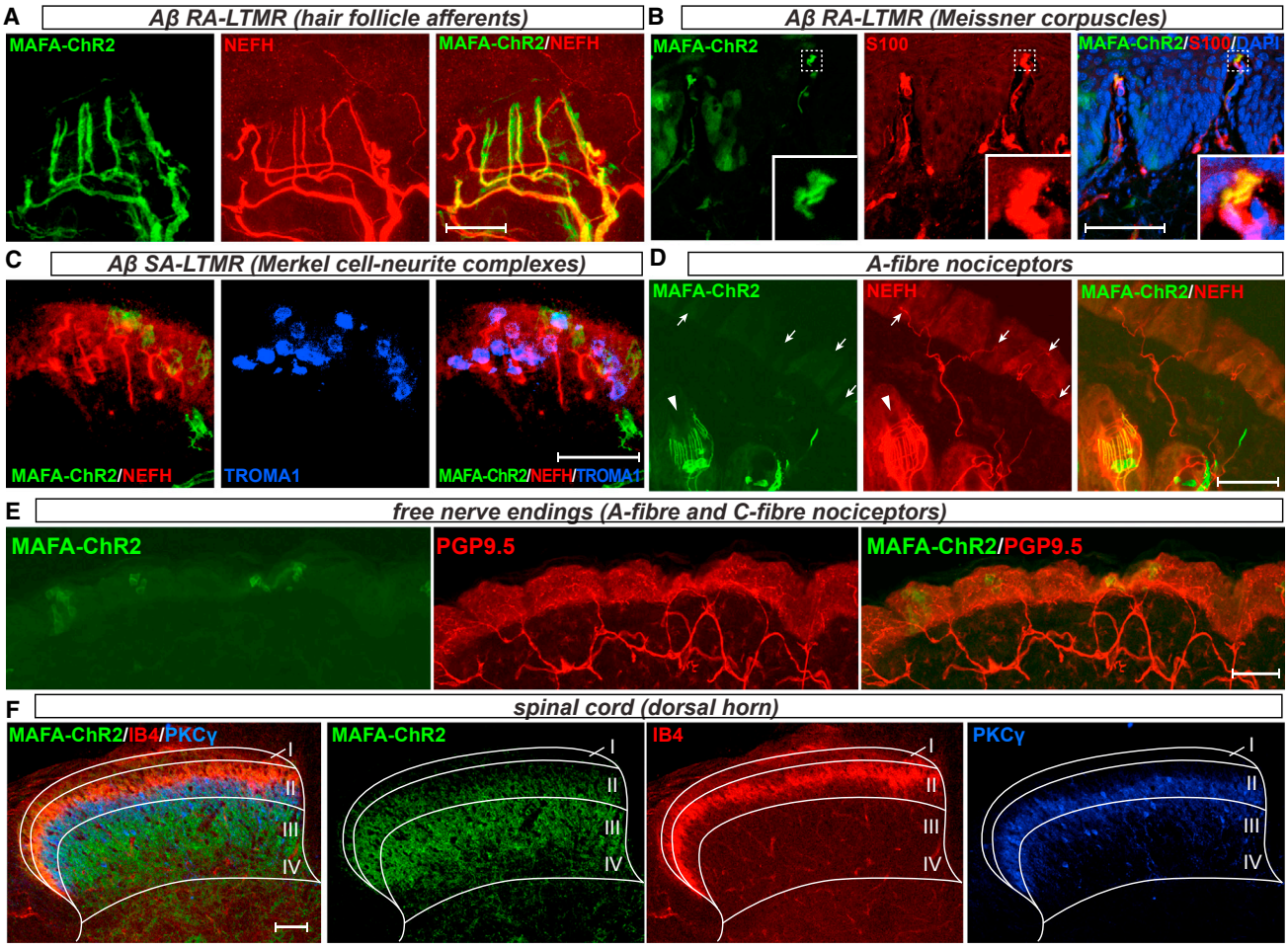

Figure 6. MafA-ChR2-Positive Afferents Innervate Mechanosensory End Organs of LTMRs

(A) MAFA-ChR2-positive (green) fibers form Nefh+ (red) lanceolate endings around hair follicles (also see D and Figure S4B).

(B) S100-positive Meissner corpuscles (red) that reside in the dermal papillae of the hindpaw footpad are innervated by MAFA-ChR2-positive fibers (green).

(C) Merkel cells visualized by TROMA1 staining (blue) are innervated by NEFH+ fibers (red) that do not express ChR2 (green).

(D) A-fiber nociceptors—i.e., NEFH+ free nerve endings (red, indicated by arrows)—do not express ChR2. In the bottom left corner, ChR2-positive lanceolate endings can be seen.

(E) Anti-PGP9.5, which labels all sensory afferents, was used to visualize free nerve endings, both myelinated (A-fiber nociceptors) and unmyelinated (C-fiber nociceptors). Note that none of the free nerve endings expressed ChR2.

(F) MAFA-ChR2-positive fibers (green) project to lamina III-IV of the spinal dorsal horn. Lamina IIo was visualized by IB4 staining (red). PKCγ staining (blue) was used to visualize the border between lamina II and III.

Scale bars, 10 (A), 50 (B–E), and 100 μm (D).

differences; Aβ RA-LTMRs and Aβ SA-LTMRs, for example, have identical CVs but fundamentally different response properties, and the same is true for low-threshold C-fibers (C-LTMRs) and C-fiber nociceptors (Abraira and Ginty, 2013; Lewin and Moshourab, 2004). Indeed, our results show that the CV distribution of NPY2R-ChR2-positive A-fiber mechanonociceptors overlaps with the distribution of the more slowly conducting ChR2-negative A-fiber mechanonociceptors (7 from 23 afferents) and at the upper end extends beyond the 10 m/s CV cutoff for Aδ-fibers (8 from 23 examined afferents), yet our data show that NPY2R-ChR2-positive nociceptors constitute a functionally and molecularly homogeneous subpopulation of A-fiber mechanonociceptors.

Our findings are strongly supported by a recent large-scale single-cell RNA sequencing study that describes *Npy2r* expression in a subset of A-fiber nociceptors (Usoskin et al., 2015). Consistent with our observation that NPY2R-Chr2-positive A-fiber mechanonociceptors have significantly faster CVs than ChR2-negative A-fiber mechanonociceptors (Figure 1C), the raw data from Usoskin et al. also reveal that *Npy2r*-expressing A-fiber nociceptors have more than 2-fold higher expression levels of neurofilament-heavy polypeptide and neurofilament-medium peptide, which are the major determinants of axon diameter and thus CV (Hoffman et al., 1987). Our results are further supported by a previous report showing that *Npy2r* is expressed in medium to large diameter CGRP-positive nociceptors

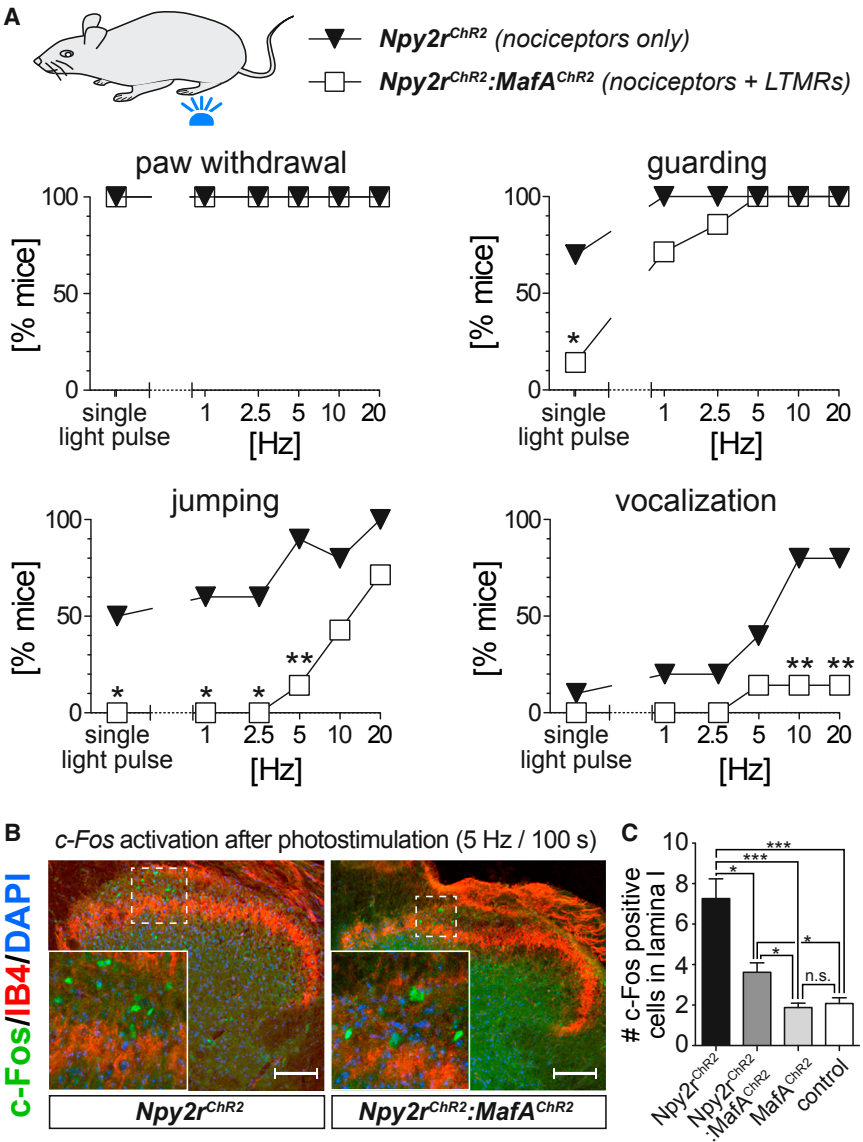

Figure 7. LTMR-Derived Sensory Input Alleviates A-Fiber Nociceptor-Evoked Pain

(A) Incidence of the indicated behavior (percent of mice showing the behavior) in response to selective photoactivation of A-fiber nociceptors (*Npy2r*^{ChR2}, black triangles; N = 10 mice) and to concurrent activation of nociceptors and LTMRs (*Npy2r*^{ChR2};*MafA*^{ChR2}, white squares; N = 7 mice) as a function of stimulation frequency. Each mouse was stimulated for 10 s. *p < 0.05; **p < 0.01; Fisher's exact test.

(B) Activation of the immediate early gene *c-Fos* visualized with immunostaining following in vivo 5 Hz photostimulation of the hindpaw of *Npy2r*^{ChR2} mice (left image) and *Npy2r*^{ChR2};*MafA*^{ChR2} mice (right image). Inset shows magnified view of the area marked with the dashed white square. Lamina IIo was visualized by IB4 staining. Scale bars, 100 μm.

(C) Quantification of *c-Fos* immunostainings after in vivo photostimulation. Numbers of *c-Fos*-positive neurons were compared using one-way ANOVA with Dunn's multiple comparison test.

in lumbar rat DRGs (Zhang et al., 1997). Furthermore, several studies showed that intrathecal administration of the NPY2R ligand NPY has an anti-nociceptive effect (Intondi et al., 2008; Solway et al., 2011; Xu et al., 1994) and it was shown that NPY suppresses excitatory postsynaptic currents (EPSCs) in substantia gelatinosa neurons via activation of NPY2R on the central terminals of primary afferents (Moran et al., 2004).

At first glance, our results differ from a previous report by Li and colleagues (2011), who showed that GFP-positive sensory afferents in an *Npy2r*^{GFP} BAC-transgenic reporter mouse line form lanceolate endings around hair follicles, which is characteristic of Aβ-fiber RA-LTMRs. Li et al., however, examined hairy back skin of the trunk, which contains hair types that are not present in the paw skin. Indeed, we also observed NPY2R-ChR2-positive lanceolate endings around guard hairs in back skin sections (Figures S3A and S3B), though we found numerous additional NPY2R-ChR2-positive fibers that terminate as free nerve endings (Figure S3A). Guard hairs are absent from the paw skin, which would explain why we never encountered light-sensitive RA-LTMRs in skin-nerve recordings and hardly observed any ChR2$^+$ RA-LTMRs in L3-L5 lumbar DRGs, which predominantly innervate the paw skin, and why Li et al. found many NPY2R-GFP-positive RA-LTMR neurons in thoracic DRGs, which exclusively innervate the trunk skin. The few putative NPY2R$^+$ RA-LTMRs (calbindin$^+$/ChR2$^+$ neurons) that we found in lumbar DRGs (Figure 2G) may represent neurons that innervate the skin covering the leg, which is anatomically identical to the back skin and also contains guard hairs. A possible explanation for why NPY2R-GFP-positive free nerve endings have not been described in the *Npy2r*^{GFP} reporter line is that Li et al. have visualized peripheral projections using whole mount skin stainings, in which free nerve endings are difficult to identify. Indeed Li et al. show that their NPY2R-GFP-positive population is heterogeneous, as more than 50% of the thoracic NPY2R-GFP positive neurons do not express c-Ret, which is found in all RA-LTMRs (Luo et al., 2009). Another possibility is that unlike the *Npy2r*^{GFP} reporter line, the *Npy2r*^{Cre} driver line also captures neurons that only transiently express *Npy2r* during development. Although the above-mentioned studies strongly argue against this theory (Usoskin et al., 2015; Zhang et al., 1997), we tested this hypothesis by comparing *Npy2r* mRNA expression levels in samples of NPY2R-ChR2-positive cells and MAFA-ChR2-positive cells using qPCR. *Npy2r* expression levels were ~5-fold higher in lumbar NPY2R-ChR2-positive neurons compared to samples containing equal numbers of MAFA-ChR2-positive cells (Figure S2C). Considering that the

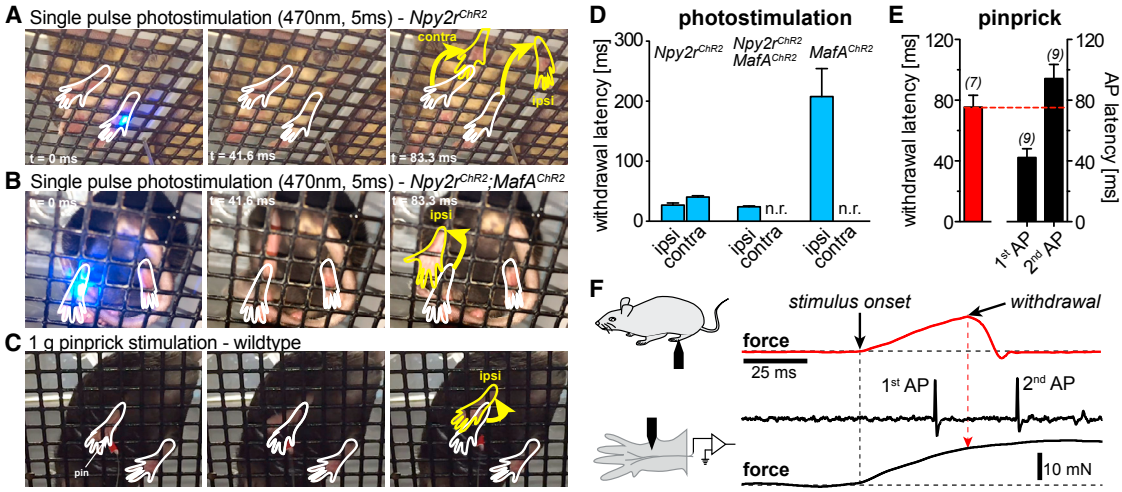

Figure 8. Concurrent Activation of A-Fiber Nociceptors and LTMRs Is Required for Well-Coordinated Withdrawal Reflex Execution

(A–C) Freeze-frame series from Movies S4 (A), S5 (B), and S1 (C) illustrating the motion sequence of paw withdrawals evoked by the indicated stimuli. Hindpaw positions before stimulation are outlined in white and positions 83.3 ms after stimulation in yellow.

(D) Mean latencies ± SEM of ipsilateral (ipsi) and contralateral (contra) paw withdrawals evoked by a single 5 ms light pulse (blue). Note that *Npy2r*^{ChR2} (N = 10) and *Npy2r*^{ChR2};*MafA*^{ChR2} (N = 7) mice responded to each stimulus (100%) with rapid paw withdrawal, whereas *MafA*^{ChR2} mice (N = 7) only occasionally responded to photostimulation (61% of the trials) and with about ten times longer latencies (n.r., no response).

(E) The left panel shows the mean ± SEM latencies of pinprick-evoked paw withdrawals, which were determined using a custom-built force measurement system that measures the force acting on the pin (see Figure S7). The right panel shows the mean ± SEM latencies of the first (1st AP) and the second action potential (2nd AP) evoked by pinprick stimuli applied with the same force and the same velocity. N numbers are indicated in brackets.

(F) Example traces of the recordings quantified in (E). Top trace shows an example of a force recording during pinprick-evoked paw withdrawals (additional examples are shown in Figure S7). Bottom traces show APs elicited by pinprick stimuli applied with the same force and the same velocity in skin-nerve recordings. Note that when the pin contacts the skin, the force starts to increase (stimulus onset) and as soon as the mouse withdraws the paw (withdrawal), the force readout returns to baseline. Also note that the second AP of pinprick-evoked spike trains is fired after the mouse withdraws the paw (see E for mean latencies) and thus cannot contribute to the initiation of paw withdrawal.

lumbar NPY2R-ChR2 population contains much less putative RA-LTMRs than the lumbar MAFA-ChR2 population (compare proportion of calbindin^{+} neurons in Figures 2G and 5F), this result suggests that NPY2R-ChR2-positive A-fiber mechanonociceptors, which account for the majority of cells in lumbar NPY2R-ChR2-positive samples, also express *Npy2r* in adult mice.

Hence, we conclude that the population of NPY2R-Cre-positive neurons captures both A-fiber nociceptors, which terminate as free nerve endings, as well as RA-LTMRs, which innervate guard hairs. Since guard hairs are, however, absent from the hairy and the glabrous paw skin, the great majority of NPY2R-ChR2 positive neurons in lumbar DRGs are A-fiber nociceptors. Accordingly, the conclusions drawn from our behavioral experiments, in which only the glabrous skin was stimulated, are not affected by this heterogeneity.

The Neural Basis of Pinprick-Evoked Paw Withdrawal

The primary function of paw withdrawal reflexes is to protect the organism from tissue damage by potentially harmful stimuli. Considering the fast axonal CVs (fastest of all nociceptors), the high mechanical thresholds, and the vigorous firing during the initial phase of noxious skin indentation (Figure 1), *Npy2r*^{Cre}-positive afferents appear to be best suited to ensure rapid and efficient execution of such reflexes. Indeed, mice lacking *Npy2r*^{Cre}-positive fibers show markedly delayed pinprick-evoked withdrawal responses (Figure 4B). The fact that these animals do not completely lose their sensitivity to pinprick stimuli can be explained by activation of unmyelinated slowly conducting C-fiber nociceptors, which are still fully functional after ablation of *Npy2r*^{Cre}-positive A-fiber mechanonociceptors. Indeed, humans, in which all A-fibers (nociceptors and LTMRs) had been blocked by nerve compression but C-fibers had been left intact, show similarly delayed responses to pinprick stimuli (Henrich et al., 2015).

Furthermore, our data suggest that pinprick-evoked paw withdrawals are not triggered by temporal summation of multiple APs from the same fiber (i.e., they are triggered independently of firing frequency), but are most likely triggered by spatial summation of single APs from multiple fibers. This hypothesis is supported by the following observations: first, we show that a 5 ms light pulse evokes only a single AP in skin-nerve recordings (Figure S4). When applied to the plantar surface of the hindpaw of awake mice, the very same 5 ms light pulse is sufficient to trigger rapid paw withdrawal (Figure 8D), suggesting that temporal summation of consecutively fired APs from the same fiber is not required to trigger paw withdrawal. However, given the size of the photostimulated area (2–3 mm diameter), it is possible that spatial summation of single APs from multiple Npy2r-positive afferents is important.

To further test this hypothesis, we measured the latencies of pinprick-evoked paw withdrawals and compared them to the latencies of the first and the second AP evoked by the same pinprick stimuli in NPY2R-positive fibers (Figures 8 and S7).

This analysis revealed that the second AP (94.2 ± 27.9 ms latency) is only fired after the paw begins to move (75.3 ± 15.6 ms) and is thus unlikely to be required for triggering nociceptive paw withdrawal (Figures 8E, 8F, and S7B). It is, however, important to note that a direct statistical comparison of AP latencies and paw withdrawal latencies would not be appropriate. Paw withdrawal inevitably occurs with a delay, the duration of which—in case of a spinal reflex—is determined by the speed of the signaling events that relay sensory information from the peripheral nerve terminal via the spinal cord to the neuromuscular junction. Our photostimulation experiments suggest that these signaling events take approximately 20 ms, which is the delay between photostimulation-evoked AP latencies (3.1 ± 0.8 ms; data not shown) and photostimulation-evoked paw withdrawal latencies (24.3 ms; Figure 8D). Indeed, this value is similar to an approximation based on theoretical considerations. Thus, AP propagation along the peripheral nerve—assuming an average nerve length of 50 mm and considering the mean CV of NPY2R$^+$ afferents (8.5 m/s; Figure 1C)—takes about 6 ms. Signal transmission from the central terminals of Npy2r$^+$ neurons to motor neurons in the ventral horn takes another ~2 ms (assuming a polysynaptic connection with at least two synapses). Finally, APs are propagated along motor efferents (~2 ms) followed by excitation-contraction coupling, which in mice takes up to 10 ms (Baylor and Hollingworth, 2003, 2012). Hence, if the second AP were required for triggering paw withdrawal, then one would expect paw withdrawal latencies to be in the range of 114 ms (94 ms second AP latency + 20 ms signaling duration). This is, however, not the case. Instead, the latencies of pinprick-evoked paw withdrawals (75.3 ms; Figures 8E and S7B) are in a range that would be expected for a single AP-dependent mechanism (~62 ms; i.e., 42 ms AP latency + 20 ms signaling duration). Hence, we propose that pinprick-evoked paw withdrawals are triggered by spatial summation of multiple single APs from multiple simultaneously activated NPY2R-positive afferents.

The Role of LTMRs in Acute Pain Signaling

Finally, our results directly demonstrate that touch receptor-derived sensory information has an analgesic effect on acute A-fiber-evoked pain and is important for nociceptive reflex encoding. A contribution of LTMRs to pain signaling had already been proposed 50 years ago by the gate control theory of pain (Melzack and Wall, 1965). The gate control theory proposed that nociceptive transmission neurons in the spinal cord receive input from both nociceptors and LTMRs; LTMR input was gated via feedforward activation of inhibitory interneurons. Indeed, numerous subsequent studies have shown that in the setting of injury, feedforward inhibition is blocked so that LTMRs can activate nociceptive transmission neurons, which results in touch-evoked pain (Braz et al., 2014; Sandkühler, 2009; Todd, 2010). However, the gate control theory further proposed that LTMRs also gate nociceptor input to transmission neurons and that increasing nociceptor activity blocks this inhibition. Our results directly confirm this important prediction; they show that LTMR input has a strong analgesic effect at low firing frequencies but hardly affects pain behavior evoked at stimulation frequencies above 5 Hz (Figure S6A). The behavioral data are strongly supported by significant differences in photostimulation-evoked c-Fos activation in neurons in lamina I of the dorsal horn (Figures 7B and 7C), which contains the majority of projection neurons that relay noxious information to higher brain regions and are therefore important for the conscious perception of pain (Braz et al., 2014; Todd, 2010). Interestingly, concurrent activation of LTMRs did not inhibit single AP-evoked paw withdrawals. Thus, LTMR input gates pain, but not nociceptive reflexes. On the contrary, LTMR input significantly improved reflex coordination. Thus, while selective activation of A-fiber mechanonociceptors evokes bilateral paw withdrawals, simultaneous activation of A-fiber mechanonociceptors and LTMRs triggers unilateral and well-coordinated paw withdrawals that are indistinguishable from reflexes evoked by natural mechanical stimuli (Figures 8B–8D; Movies S1, S4, and S5). Tactile feedback had already been proposed to be important for the refinement and functional adaptation of the nociceptive withdrawal reflex system during early postnatal development (Petersson et al., 2003; Waldenström et al., 2003), but it was hitherto unclear if it is also involved in nociceptive reflex signaling in adult mice.

Taken together, our results highlight two fundamentally different types of crosstalk between nociceptors and LTMRs. Thus, while LTMRs exert inhibitory control on acute mechanical pain signaling (Figure 7A), presumably at the level of the spinal dorsal horn (Figure 7B), they have a positive modulatory function that is required for the normal and well-coordinated execution of nocifensive reflexes (Figures 8A and 8B).

Conclusions

In summary, our study reveals the importance of touch receptors in pain signaling and, for the first time, establishes a causal link between precisely defined neural activity in genetically identified sensory neuron subpopulations and nocifensive behavior and pain. Moreover, in identifying and characterizing Cre-driver lines that allow the selective manipulation of LTMR and A-fiber nociceptor function, our results provide an invaluable framework for future studies that aim to dissect the neural circuits in the spinal cord that process and integrate tactile and noxious information.

EXPERIMENTAL PROCEDURES

Animals

The following mouse lines were used: *Npy2r*$^{Cre/+}$ (Tg(Npy2r-cre)SM19Gsat/Mmucd; RRID: MMRRC_036630-UCD), *ChR2*$^{loxP/+}$ (B6;129S-Gt(ROSA)26Sortm32(CAG-COP4*H134R/EYFP)Hze/J; RRID: IMSR_JAX:012569), Z/AP reporter mice (B6;129-lis1tm3(CAG-Bgeo,-tdTomato/TEVP,-DLG,-GFP)Nat/J; RRID: IMSR_JAX:003919), *Avil*^{iDTR} (RRID: IMSR_EM:10409), and *MafA*^{Cre} mice (Figure S5). Additional information is provided in the Supplemental Experimental Procedures.

Immunohistochemistry

A detailed description of the immunostaining protocols and the antibodies that were used is provided in the Supplemental Experimental Procedures.

In Vitro Skin-Nerve Preparation

The skin-nerve preparation was used as previously described (Heidenreich et al., 2011; Koltzenburg et al., 1997). Mice 8–12 weeks old were sacrificed, and the sural nerve and the skin of the hindlimb were dissected free and placed in a heated (32°C) organ bath, perfused with synthetic interstitial fluid (see

Supplemental Experimental Procedures for composition). The skin was placed with the corium side up in the organ bath and the nerve was placed in an adjacent chamber for fiber teasing and single-unit recording. Single units were isolated with a mechanical search stimulus applied with a glass rod and classified by CV, von Frey hair thresholds, and adaptation properties to suprathreshold stimuli (Koltzenburg et al., 1997). Mechanical ramp-and-hold stimuli were applied with a Nanomotor. Photostimuli were generated by a laser (470 nm, Shanghai Laser & Optics Century) and were applied to the skin via a light guide (FG910UEC, Thorlabs) that was coupled to a 20× microscope objective using a custom-made adaptor, which allowed us to precisely focus the light onto a small skin area. Light-pulse duration and frequency were controlled by an external trigger generated by the stimulator function of LabChart 7.1 (AD Instruments). Raw electrophysiological data were recorded with a Powerlab 4SP system and Labchart 7.1 software, and spikes were discriminated offline with the spike histogram extension of the software. Additional details are provided in the Supplemental Experimental Procedures.

Primary DRG Cultures and Patch-Clamp Recordings

The preparation of primary DRG cultures and the protocol of patch-clamp recordings are described in the Supplemental Experimental Procedures.

Behavioral Assays

Behavioral tests were carried out in accordance with ethical guidelines imposed by the local governing body (Regierungspraesidium Karlsruhe, Germany) in awake, unrestrained, age-matched mice (8 and 12 weeks old). All tests were performed in a quiet room between 11 a.m. and 4 p.m. Animals were kept in individual cages on a 12 hr light-dark cycle with constant room temperature.

Mice were placed on a perforated metal platform inside transparent plastic cubicles (Ugo Basile) and were allowed to acclimatize to the environment for 60 min. The plantar surface of the hindpaw was stimulated through the holes of the metal platform using a 1 g von Frey filament (von Frey test), dissecting pin glued to the tip of a 1 g von Frey filament (pinprick test), and photostimuli. Photostimuli were generated and applied with the device described above (see in vitro skin-nerve preparation). Light intensities were measured with a PM100D powermeter (Thorlabs). All trials were filmed at a frame rate of 240 fps (4.16 ms per frame) using an iPhone6 (Apple). Withdrawal latencies shown in Figure 4B were determined by counting the number of frames between onset of the stimulus and movement of the paw. Withdrawal latencies in response to pinprick and von Frey stimuli shown in Figures 8A and S7B were measured using a custom-made force measurement system (Figure S7A; PL-FMS-EM000, Kleindiek Nanotechnik). The hot plate test was performed with a hot/cold plate (Bioseb) at 55°C. The latency until the first withdrawal response of the hindpaw was measured and mice were removed immediately.

DTX-Induced Ablation

To ablate NPY2R-positive sensory neurons, *Npy2r*^{iDTR} and control mice were injected intraperitoneally twice with 40 μg/kg DTX (Sigma D0564) over a 72 hr time interval. Behavioral experiments were performed 7 days after the second DTX injection.

Reverse Transcription and Quantitative Real-Time PCR

A detailed description of how Npy2r expression levels were measured is provided in the Supplemental Experimental Procedures.

SUPPLEMENTAL INFORMATION

Supplemental Information includes Supplemental Experimental Procedures, seven figures, and six movies and can be found with this article online at http://dx.doi.org/10.1016/j.neuron.2016.11.027.

AUTHOR CONTRIBUTIONS

Conceptualization, S.G.L.; Investigation, A.A., L.G., R.D., F.J.T., V.P., H.W., V.G., and S.G.L.; Methodology, V.G., P.A.H., C.B., and S.G.L.; Formal Analysis, A.A., L.G., R.D., and S.G.L.; Writing, S.G.L.; Funding Acquisition, P.A.H. and S.G.L.

ACKNOWLEDGMENTS

This study was supported by DFG grants LE3210-1 and SFB1158/1 to S.G.L. and SFB1158/2 to P.A.H. We thank Ms. Anke Niemann and Ms. Nadine Gehrig for technical assistance and Prof. Rohini Kuner for fruitful discussions and generous sharing of equipment, which furthered progress of the study, and Prof. Jan Siemens for providing the Trpv1 antibody.

Received: February 23, 2016
Revised: August 1, 2016
Accepted: November 7, 2016
Published: December 15, 2016

REFERENCES

Abraira, V.E., and Ginty, D.D. (2013). The sensory neurons of touch. Neuron *79*, 618–639.

Akopian, A.N., Souslova, V., England, S., Okuse, K., Ogata, N., Ure, J., Smith, A., Kerr, B.J., McMahon, S.B., Boyce, S., et al. (1999). The tetrodotoxin-resistant sodium channel SNS has a specialized function in pain pathways. Nat. Neurosci. *2*, 541–548.

Averill, S., McMahon, S.B., Clary, D.O., Reichardt, L.F., and Priestley, J.V. (1995). Immunocytochemical localization of trkA receptors in chemically identified subgroups of adult rat sensory neurons. Eur. J. Neurosci. *7*, 1484–1494.

Bai, L., Lehnert, B.P., Liu, J., Neubarth, N.L., Dickendesher, T.L., Nwe, P.H., Cassidy, C., Woodbury, C.J., and Ginty, D.D. (2015). Genetic identification of an expansive mechanoreceptor sensitive to skin stroking. Cell *163*, 1783–1795.

Basbaum, A.I., Bautista, D.M., Scherrer, G., and Julius, D. (2009). Cellular and molecular mechanisms of pain. Cell *139*, 267–284.

Baylor, S.M., and Hollingworth, S. (2003). Sarcoplasmic reticulum calcium release compared in slow-twitch and fast-twitch fibres of mouse muscle. J. Physiol. *551*, 125–138.

Baylor, S.M., and Hollingworth, S. (2012). Intracellular calcium movements during excitation-contraction coupling in mammalian slow-twitch and fast-twitch muscle fibers. J. Gen. Physiol. *139*, 261–272.

Bourane, S., Garces, A., Venteo, S., Pattyn, A., Hubert, T., Fichard, A., Puech, S., Boukhaddaoui, H., Baudet, C., Takahashi, S., et al. (2009). Low-threshold mechanoreceptor subtypes selectively express MafA and are specified by Ret signaling. Neuron *64*, 857–870.

Braz, J., Solorzano, C., Wang, X., and Basbaum, A.I. (2014). Transmitting pain and itch messages: a contemporary view of the spinal cord circuits that generate gate control. Neuron *82*, 522–536.

Cain, D.M., Khasabov, S.G., and Simone, D.A. (2001). Response properties of mechanoreceptors and nociceptors in mouse glabrous skin: an in vivo study. J. Neurophysiol. *85*, 1561–1574.

Caterina, M.J., Schumacher, M.A., Tominaga, M., Rosen, T.A., Levine, J.D., and Julius, D. (1997). The capsaicin receptor: a heat-activated ion channel in the pain pathway. Nature *389*, 816–824.

Del Barrio, M.G., Bourane, S., Grossmann, K., Schüle, R., Britsch, S., O'Leary, D.D.M., and Goulding, M. (2013). A transcription factor code defines nine sensory interneuron subtypes in the mechanosensory area of the spinal cord. PLoS ONE *8*, e77928.

Djouhri, L., and Lawson, S.N. (2004). Abeta-fiber nociceptive primary afferent neurons: a review of incidence and properties in relation to other afferent A-fiber neurons in mammals. Brain Res. Brain Res. Rev. *46*, 131–145.

Duan, B., Cheng, L., Bourane, S., Britz, O., Padilla, C., Garcia-Campmany, L., Krashes, M., Knowlton, W., Velasquez, T., Ren, X., et al. (2014). Identification of spinal circuits transmitting and gating mechanical pain. Cell *159*, 1417–1432.

Dubin, A.E., and Patapoutian, A. (2010). Nociceptors: the sensors of the pain pathway. J. Clin. Invest. *120*, 3760–3772.

Ernfors, P., Lee, K.F., Kucera, J., and Jaenisch, R. (1994). Lack of neurotrophin-3 leads to deficiencies in the peripheral nervous system and loss of limb proprioceptive afferents. Cell *77*, 503–512.

Georges-Labouesse, E., Messaddeq, N., Yehia, G., Cadalbert, L., Dierich, A., and Le Meur, M. (1996). Absence of integrin alpha 6 leads to epidermolysis bullosa and neonatal death in mice. Nat. Genet. *13*, 370–373.

Heidenreich, M., Lechner, S.G., Vardanyan, V., Wetzel, C., Cremers, C.W., De Leenheer, E.M., Aránguez, G., Moreno-Pelayo, M.Á., Jentsch, T.J., and Lewin, G.R. (2011). KCNQ4 K(+) channels tune mechanoreceptors for normal touch sensation in mouse and man. Nat. Neurosci. *15*, 138–145.

Henrich, F., Magerl, W., Klein, T., Greffrath, W., and Treede, R.-D. (2015). Capsaicin-sensitive C- and A-fibre nociceptors control long-term potentiation-like pain amplification in humans. Brain *138*, 2505–2520.

Hoffman, P.N., Cleveland, D.W., Griffin, J.W., Landes, P.W., Cowan, N.J., and Price, D.L. (1987). Neurofilament gene expression: a major determinant of axonal caliber. Proc. Natl. Acad. Sci. USA *84*, 3472–3476.

Intondi, A.B., Dahlgren, M.N., Eilers, M.A., and Taylor, B.K. (2008). Intrathecal neuropeptide Y reduces behavioral and molecular markers of inflammatory or neuropathic pain. Pain *137*, 352–365.

Koltzenburg, M., Stucky, C.L., and Lewin, G.R. (1997). Receptive properties of mouse sensory neurons innervating hairy skin. J. Neurophysiol. *78*, 1841–1850.

Lawson, J.J., McIlwrath, S.L., Woodbury, C.J., Davis, B.M., and Koerber, H.R. (2008). TRPV1 unlike TRPV2 is restricted to a subset of mechanically insensitive cutaneous nociceptors responding to heat. J. Pain *9*, 298–308.

Lechner, S.G., and Lewin, G.R. (2013). Hairy sensation. Physiology (Bethesda) *28*, 142–150.

Lewin, G.R., and Moshourab, R. (2004). Mechanosensation and pain. J. Neurobiol. *61*, 30–44.

Li, L., Rutlin, M., Abraira, V.E., Cassidy, C., Kus, L., Gong, S., Jankowski, M.P., Luo, W., Heintz, N., Koerber, H.R., et al. (2011). The functional organization of cutaneous low-threshold mechanosensory neurons. Cell *147*, 1615–1627.

Luo, W., Enomoto, H., Rice, F.L., Milbrandt, J., and Ginty, D.D. (2009). Molecular identification of rapidly adapting mechanoreceptors and their developmental dependence on ret signaling. Neuron *64*, 841–856.

Ma, Q. (2010). Labeled lines meet and talk: population coding of somatic sensations. J. Clin. Invest. *120*, 3773–3778.

Madisen, L., Mao, T., Koch, H., Zhuo, J.M., Berenyi, A., Fujisawa, S., Hsu, Y.-W.A., Garcia, A.J., 3rd, Gu, X., Zanella, S., et al. (2012). A toolbox of Cre-dependent optogenetic transgenic mice for light-induced activation and silencing. Nat. Neurosci. *15*, 793–802.

Maricich, S.M., Wellnitz, S.A., Nelson, A.M., Lesniak, D.R., Gerling, G.J., Lumpkin, E.A., and Zoghbi, H.Y. (2009). Merkel cells are essential for light-touch responses. Science *324*, 1580–1582.

McIlwrath, S.L., Lawson, J.J., Anderson, C.E., Albers, K.M., and Koerber, H.R. (2007). Overexpression of neurotrophin-3 enhances the mechanical response properties of slowly adapting type 1 afferents and myelinated nociceptors. Eur. J. Neurosci. *26*, 1801–1812.

Melzack, R., and Wall, P.D. (1965). Pain mechanisms: a new theory. Science *150*, 971–979.

Milenkovic, N., Wetzel, C., Moshourab, R., and Lewin, G.R. (2008). Speed and temperature dependences of mechanotransduction in afferent fibers recorded from the mouse saphenous nerve. J. Neurophysiol. *100*, 2771–2783.

Mogil, J.S. (2009). Animal models of pain: progress and challenges. Nat. Rev. Neurosci. *10*, 283–294.

Molliver, D.C., Wright, D.E., Leitner, M.L., Parsadanian, A.S., Doster, K., Wen, D., Yan, Q., and Snider, W.D. (1997). IB4-binding DRG neurons switch from NGF to GDNF dependence in early postnatal life. Neuron *19*, 849–861.

Moran, T.D., Colmers, W.F., and Smith, P.A. (2004). Opioid-like actions of neuropeptide Y in rat substantia gelatinosa: Y1 suppression of inhibition and Y2 suppression of excitation. J. Neurophysiol. *92*, 3266–3275.

Petersson, P., Waldenström, A., Fåhraeus, C., and Schouenborg, J. (2003). Spontaneous muscle twitches during sleep guide spinal self-organization. Nature *424*, 72–75.

Prescott, S.A., Ma, Q., and De Koninck, Y. (2014). Normal and abnormal coding of somatosensory stimuli causing pain. Nat. Neurosci. *17*, 183–191.

Rutlin, M., Ho, C.-Y., Abraira, V.E., Cassidy, C., Bai, L., Woodbury, C.J., and Ginty, D.D. (2014). The cellular and molecular basis of direction selectivity of Aδ-LTMRs. Cell *159*, 1640–1651.

Sandkühler, J. (2009). Models and mechanisms of hyperalgesia and allodynia. Physiol. Rev. *89*, 707–758.

Solway, B., Bose, S.C., Corder, G., Donahue, R.R., and Taylor, B.K. (2011). Tonic inhibition of chronic pain by neuropeptide Y. Proc. Natl. Acad. Sci. USA *108*, 7224–7229.

Sonnenberg, A., Calafat, J., Janssen, H., Daams, H., van der Raaij-Helmer, L.M., Falcioni, R., Kennel, S.J., Aplin, J.D., Baker, J., Loizidou, M., et al. (1991). Integrin alpha 6/beta 4 complex is located in hemidesmosomes, suggesting a major role in epidermal cell-basement membrane adhesion. J. Cell Biol. *113*, 907–917.

Stantcheva, K.K., Iovino, L., Dhandapani, R., Martinez, C., Castaldi, L., Nocchi, L., Perlas, E., Portulano, C., Pesaresi, M., Shirlekar, K.S., et al. (2016). A subpopulation of itch-sensing neurons marked by Ret and somatostatin expression. EMBO Rep. *17*, 585–600.

Stucky, C.L., Koltzenburg, M., Schneider, M., Engle, M.G., Albers, K.M., and Davis, B.M. (1999). Overexpression of nerve growth factor in skin selectively affects the survival and functional properties of nociceptors. J. Neurosci. *19*, 8509–8516.

Todd, A.J. (2010). Neuronal circuitry for pain processing in the dorsal horn. Nat. Rev. Neurosci. *11*, 823–836.

Usoskin, D., Furlan, A., Islam, S., Abdo, H., Lönnerberg, P., Lou, D., Hjerling-Leffler, J., Haeggström, J., Kharchenko, O., Kharchenko, P.V., et al. (2015). Unbiased classification of sensory neuron types by large-scale single-cell RNA sequencing. Nat. Neurosci. *18*, 145–153.

Waldenström, A., Thelin, J., Thimansson, E., Levinsson, A., and Schouenborg, J. (2003). Developmental learning in a pain-related system: evidence for a cross-modality mechanism. J. Neurosci. *23*, 7719–7725.

Wende, H., Lechner, S.G., Cheret, C., Bourane, S., Kolanczyk, M.E., Pattyn, A., Reuter, K., Munier, F.L., Carroll, P., Lewin, G.R., and Birchmeier, C. (2012). The transcription factor c-Maf controls touch receptor development and function. Science *335*, 1373–1376.

Woodbury, C.J., and Koerber, H.R. (2003). Widespread projections from myelinated nociceptors throughout the substantia gelatinosa provide novel insights into neonatal hypersensitivity. J. Neurosci. *23*, 601–610.

Wu, H., Williams, J., and Nathans, J. (2012). Morphologic diversity of cutaneous sensory afferents revealed by genetically directed sparse labeling. eLife *1*, e00181.

Xu, X.J., Hao, J.X., Hökfelt, T., and Wiesenfeld-Hallin, Z. (1994). The effects of intrathecal neuropeptide Y on the spinal nociceptive flexor reflex in rats with intact sciatic nerves and after peripheral axotomy. Neuroscience *63*, 817–826.

Zhang, X., Shi, T., Holmberg, K., Landry, M., Huang, W., Xiao, H., Ju, G., and Hökfelt, T. (1997). Expression and regulation of the neuropeptide Y Y2 receptor in sensory and autonomic ganglia. Proc. Natl. Acad. Sci. USA *94*, 729–734.